

# Inkwell: Design and Validation of a Low-Cost Open Electricity-Free 3D Printed Device for Automated Thin Smearing of Whole Blood

Jerome Nowak<sup>1,†</sup>, Anesta Kothari<sup>2,†</sup>, Hongquan Li<sup>3</sup>, Jaspreet Pannu<sup>4</sup>, Dani  
Algazi<sup>5</sup>, and Manu Prakash<sup>2,6,7,8,\*</sup>

<sup>1</sup>Department of Mechanical Engineering

<sup>2</sup>Department of Bioengineering

<sup>3</sup>Department of Electrical Engineering

<sup>4</sup>Department of Medicine

<sup>5</sup>Department of Computer Science

<sup>6</sup>Department of Biology(courtesy)

<sup>7</sup>Woods Institute of the Environment

<sup>8</sup>Center for Innovation in Global Health

<sup>1</sup>Stanford University, Stanford, California, USA

<sup>†</sup>co-first author

\*To whom correspondence should be addressed: manup@stanford.edu

April 21, 2023

## ABSTRACT

Microscopy plays a crucial role in hematology and diagnosis of infectious diseases worldwide. For malaria alone, more than 200 million slides are read by manual microscopists every year. High quality thin blood smears are essential for subsequent microscopy examinations including malaria microscopy, but are hard to make in field settings. Current manual smearing methods lack consistency and often do not provide a uniformly dense mono-layer of red blood cells, even when prepared by trained experts. Existing devices for assisting in making thin smears are available but are limited by cost or complexity for wider use. Here we present Inkwell, a portable mechanical device capable of making high quality thin blood smears in field settings. Inkwell is simple, low-cost, does not use electricity, and requires minimal training prior to use. By utilizing passive dissipative dynamics of a spiral spring coupled to an air dashpot with a tunable valve - we demonstrate a highly tunable mechanism for constant velocity smears at prescribed angle. Inkwell is capable of producing high quality blood smears of tunable cell density with more than 12 million individually distinguishable red blood cells on a single slide. The current design, which exploits precision manufacturing of a 17 cents plastic syringe and a spring, can be printed on a standard 3D printer with overall unit cost of less than a few dollars in large quantities. We further present usability tests to confirm performance over 10,000 unit cycle operations with no degradation in quality of the smear and demonstrate ease of use with minimal training. Inkwell enhances the broader toolbox of open innovations in diagnostics for providing high quality medical care in low and medium resource settings. Combined with rise of 3D printing, Inkwell presents an alternative to traditional centralized manufacturing and opens up distributed manufacturing of medical diagnostics in global context.

**Keywords:** Malaria diagnostics, microscopy

# 1 Introduction

A single drop of finger prick blood from a patient contains over 10 million blood cells. Traditionally, this drop of blood (roughly 2-4  $\mu\text{l}$  in volume) is spread across a glass slide as a thin film, commonly referred to as a “thin blood smear”. As a standard practice in hematology, thin smears are used across clinical diagnostics including the current gold standard test for malaria diagnosis. Across primary, secondary and tertiary hospitals around the world, a patient finger prick blood based thin smear is fixed, stained and placed under a microscope to identify a number of parasites including malaria, [1] but also babesia, loa loa, microfilariae and trypanosomes. Detecting malaria parasites early and identifying species with accuracy and sensitivity is key to controlling the disease. The ability to do this depends highly on the quality of the smears and staining [2, 3] and the skill of the microscopist [4]. In particular, in many cases it is essential to have clear views of a single layer of red blood cells (RBCs), called the monolayer. Indeed this monolayer is useful firstly for identifying species to monitor the disease [5] and secondly to diagnose late stages of infections when the parasitemia is high. Furthermore, there is a rise of automated microscopes and computer-vision based parasitemia measurement [6, 7], which require consistent thin smear preparation and large monolayers of individual red blood cells for effective model training and good detection performance.

However, smears produced in labs and in the field vary widely in quality due to lack of training and poor conditions for making the smears [2, 8, 9, 10, 11], which constitutes a hindrance to manual diagnosis and a barrier to automated diagnosis. Field collection of blood smears also plays an integral role in quality management, where smears are collected and centrally stored for later evaluation. Low quality smears significantly affect the functioning of any of these quality control programs. Often in remote field sites, healthcare workers need to collect and smear blood samples outside on the ground, without a stable horizontal surface on which to work [Fig. 1a, b]. The variability is seen in the thickness, length, symmetry, uniformity, and position of the blood film, among other aspects [Fig. 1b, d]. Even after a

long training period, most health care workers find it difficult to make perfect thin-smears, specially in primary health care and field settings [Fig. 1a, b].

Conventional smearing methods typically involve 2 glass slides: a sample slide and a spreader slide. A drop of blood is deposited onto the sample slide, then the spreader slide is brought in contact with the droplet at an angle typically between  $30^\circ$  and  $45^\circ$  such that a meniscus spanning the whole width of the slide is formed between the two glass slides. While the sample slide remains stationary, the spreader slide is pushed away from the meniscus tail to form a thin blood smear on the sample slide [12, 13, 14] [Fig. 1c]. The various parameters linked to how the technician holds and moves the spreader slide, including angle of inclination, velocity and direction of motion, and whether full contact between the two slides remains constant lead to the high variability seen in smears made by hand and in the field. If the spreader slide is pushed in the other direction, towards the blood meniscus; blood cells can be sheared leading to unwanted cell lysis.

Within a single conventional smear made by hand, the thickness of deposited blood tapers down from a thick film of overlapping cells at the start to a monolayer of cells at the finish [Fig. 1f]. This ultimate “feathered edge,” a rounded, lighter colored area at the end of the smear, is often desired. Such an edge indicates symmetric pressure and motion and good wetting until the entire droplet was spread [15], resulting in a monolayer of cells ideal for parasitemia identification. What constitutes as a “good” smear is having a large zone of monolayered cells, while a “bad” smear contains largely of overlapping of cells (which makes parasite identification impossible) or an overly-sparse distribution of cells (which may not give a good representative of the sample) [Fig. 1e]. Although additional training can improve a technician’s ability to make good smears [16], having an accessible method or device that can consistently produce good smears regardless of technical skills can significantly improve the outcome of field diagnostics.

Currently, there are a few products that are commercially available which addresses this need to produce consistently good smears. The Perfect Smear tool [17] is a flexible disposable

plastic tool used as a spreader (in place of a glass slide) that can potentially produce good-quality smears with each use. However, it still relies on the technician’s experienced dexterous hands to produce a good smear. Other devices which don’t rely on technician dexterity exist on the market, like Autoslide and Hemaprep [18], however their price of hundreds to thousands of USD is prohibitive for many markets. Aside from commercial products, Autoheam is a pair of open-source devices (one manual version and the other motorized) that were recently developed to address a similar problem. However, the manual version is still not suitable for standardizing smear-making because it still relies on the user to control the velocity of the spreader slide by hand, while the motorized version requires electricity and costs over \$50 [19]. Furthermore, in the study of Autoheam[19], diluted blood instead of regular whole blood was used, limiting the direct translation of smearing parameters for clinical use. Other solutions, such as the Sysmex Hemoslider [20], have been incorporated into their proprietary automated smear and staining machine (the RAL Smearbox [21]), which can also represent a prohibitive investment. Therefore despite all the advancements, there is still no widely applicable, cost effective, efficient and accessible solution in this problem space.

Our work addresses the gap in affordable solutions to create high-quality smears without extensive technical training. In particular we focus on thin smears where at least 75% of the slide is covered in a monolayer suitable for inspection by a microscopist. Smears that contain this large coverage of monolayer are suited for emerging whole slide scanners that use computer vision for blood smear examination and quantification [6]. We first present a systematic experimental investigation of physical parameters that are optimal for creating dense monolayer smears (thin film spreading) from human whole blood. This provides a good understanding of the physical phenomena at play and helps to accurately identify the requirements for high-quality smear-making to be used in designing a cost effective and simple solutions. We then describe the complete design and evaluation of Inkwell: an open-source, low-cost, simple device that can reliably produce such smears without the need for

electricity nor extensive operator training. Utilizing a 17 cent syringe and a 3D printed parts, Inkwell can be made for a few dollars in parts and capable of smearing 12 million individual cells on a single standard glass slide. We demonstrate that Inkwell can operate for 10,000 cycles continuously without any degradation in performance.

## Results

### Observing the blood coating process

Macroscopically, there are three phases in the making of a thin blood smear. First, once contact between the drop of blood and the spreader slide occurs, capillary action spreads the drop across the wedge formed between the two static pieces of glass. Next, the spreader slide is pushed and the reservoir of blood travels with it, leaving behind a wet thin blood film whose thickness is dependent on slide angle and speed of actuation. Lastly, the wet blood film dries out with blood cells setting on the glass slide and it is ready for fixing.

Using a high-speed camera under a microscope (see Materials and Methods), we first imaged this process at high temporal and spatial resolution [Fig. 2] and supplementary video S1 A and B. It is clear from this dataset that blood cells are not immediately deposited on the slide and are floating in the fluid thin film. Two key time scales can be observed during this deposition process. Firstly, the blood reservoir traveling with the spreader slide leaves a *suspension* of cells and plasma as a thin film of specific thickness behind. Secondly, with the pull of gravity and the evaporation of plasma, the blood cells quickly settle onto the slide in the next five to thirty seconds (duration depends on the layer height, blood viscosity, and ambient temperature and humidity amongst other parameters). We visualize this process using high speed imaging and also repeat this experiment for a range of spreading velocity and total blood volume. For details see supplementary videos S1 A and B and on Fig. 2.

## Physical regime for thin film coatings

The process of depositing thin films on solid substrates has been extensively studied [22] for both Newtonian and Non-Newtonian fluids. Two regimes can be identified as a function of deposition velocity  $v_0$ : an evaporative regime at low velocities (where the coating flow is driven mainly by solvent evaporation in the liquid meniscus), and Landau-Levich regime at higher velocities (where the coating flow is mainly driven by viscous forces) [23]. From high speed imaging described above, it is clear that blood thin smear formation falls broadly in Landau-Levich [24, 25] limit with separation of time scale between evaporation (longer time scale) from deposition (shorter time scale).

Multi-scale modeling of blood hydrodynamics presents two challenges: blood is a complex non-Newtonian fluid where individual red blood cells, white blood cells and platelets are suspended in a plasma - and interact colloid where particles (red blood cells, white blood cells, and platelets) are suspended in a solvent (plasma) [26, 27]. Red blood cells (RBCs) are the most numerous particles and those of greatest interest here. Once the deposited film of blood dries, each part of the slide gets populated with the cells suspended directly above it. Assuming a homogeneous mix, this means the final surface density of RBCs on the slide after evaporation is proportionate to the thickness of the deposited fluid film. Therefore understanding what processes govern the height of the deposited thin film correlates to number of RBC per unit area.

Colloidal coating processes have been carefully studied in the evaporative regime in [28]. At typical velocities and evaporation rates, blood smearing happens in the Landau-Levich regime [29]. The latter paper provides a simple formulation for blood smearing, in the form of a Newtonian fluid in Landau-Levich regime smeared at constant velocity  $v_0$  and angle  $\phi$  between the spreader and sample slide. In steady state (i.e. infinite supply of fluid in the meniscus), the deposited film thickness is given by  $h_\infty = 1.34RCa^{2/3}$  where  $Ca = \eta v_0 / \sigma$  is the capillary number, and  $R$  the radius of the meniscus. In practice, at large timescales, the volume in the meniscus shrinks as a film is drawn from it. Assuming

quasi-steady-state and no-slip condition between the deposited film and the substrate yields  $h(x) = h_{\infty 0} - kx$  where  $x$  is the distance traveled since the beginning of the smear and  $k$  a velocity-dependent constant given by  $k(\phi, v_0) = \frac{0.898}{\tan(\frac{\pi-\phi}{2}) + \frac{\phi-\pi}{2}} (\frac{\eta v_0}{\sigma})^{4/3}$ . This means for a set velocity  $v_0$  and angle  $\phi$ , a wedge-shaped deposited film is predicted. Conservation of the volume  $V_0$  yields:  $h_{\infty 0} = \sqrt{2k(\phi, v_0)V_0/l}$  where  $l = 25$  mm is the width of the slide. Finally, the smear height is given by:  $h(x, \phi, V_0, v_0) = \sqrt{2k(\phi, v_0)\frac{V_0}{l}} - k(\phi, v_0)x$ . This model predicts that cell density increases with velocity, initial volume, and spreader angle, and that the slope of the film does not depend on the initial volume.

Given a RBC volume density of  $n_V = 4-6 \times 10^6$  cells/ $\mu$ L [30], we can infer the number of cells deposited per unit surface on the sample slide:  $n_S = n_V h$ . Furthermore, the maximum cell density without overlaps is a densely packed hexagonal lattice, with packing density  $p = \frac{\pi}{2\sqrt{3}} \approx 0.907$ , and a corresponding maximum cell density:  $n_{S,max} = \frac{p}{\pi d^2/4} \approx 18,000$  cells /  $\text{mm}^2$  where we estimated the diameter of a deposited RBC to be  $d = 8$   $\mu$ m. This means that to cover a surface  $S_{tot} = 25 \times 50$   $\text{mm}^2$  with a dense monolayer of RBCs (about 22 million), we need at least  $V_{min} = n_{S,max}/n_V \approx 3.7-5.6$   $\mu$ l of blood. This gives us a theoretical idea of appropriate volumes that would be useful to test in lab experiments.

## Finding optimal smearing parameters

In the case of high-throughput malaria microscopy, the optimal density is the highest number of RBCs on a given slide without overlapping cells. This optimum is theoretically achieved with cells closely packed in a hexagonal lattice of around 18,000 cells/ $\text{mm}^2$  (see above). Furthermore, the greater the area covered by such a dense monolayer, the more cells can be scanned in a single smear leading to higher diagnostic sensitivity in low parasitemia samples. Our goal is to find the optimal smearing parameters to maximize both cell density and slide area covered while producing little to no overlap between RBCs.

To experimentally test the parameter regime, we built a motorized smearing device and operated it at different parameters: initial blood drop volume, spreader angle, spreader



velocity, and spreader contact force (Figure S4 e-g). We first test blood droplet volumes from 2  $\mu\text{L}$  to 4  $\mu\text{L}$ , spreader angles from  $20^\circ$  to  $60^\circ$ , and smearing velocities from 5 mm/s to 50 mm/s. To quantitatively evaluate the quality of the smear - we directly image the entire slide and directly map density of cells per unit area to identify optimal driving conditions. We found that increasing the blood volume, the spreader angle or the velocity results in thicker, and therefore shorter, smears. These results concur with existing practical knowledge and preliminary theory (see section above). An overview of the smears we obtained across the entire parameter space is given [Fig. 3](#) and figure S4b.

Although the WHO recommends holding the spreader at  $30^\circ$  to  $45^\circ$  [15], we found that angles below  $30^\circ$ , where the spreader is almost parallel to the sample slide, produced much more uniform wetting across the smear. These lower angles are less practical for an operator producing conventional manual smears, but are technically possible on our automated platform. Given a constant velocity of 15-20 mm/s and initial blood volume of 4  $\mu\text{L}$ , we found  $20^\circ$  to work best (though we did not test lower angles for practical design reasons). About 3 to 6  $\mu\text{L}$  of blood is required to cover a  $50 \times 25 \text{ mm}^2$  glass slide surface with a dense monolayer of RBCs up to 18,000 cells per  $\text{mm}^2$  (see Materials and Methods). With 4  $\mu\text{L}$  of initial blood volume and a spreader angle of  $20^\circ$ , we experimentally found that velocities below 15 mm/s produced sparse spacing of cells, while velocities above 20 mm/s often produced a large zone of overlapping cells. Therefore, 15 mm/s to 20 mm/s was optimal to produce near uniform smears at densities around 9,000 to 13,000 cells/ $\text{mm}^2$  with almost no overlapping. While the simplified theory in previous work presented above predicts a constant negative gradient in cell density from the start to the end of the smear, we observed near uniform density across the entire smear, provided there is a sufficient initial volume of blood [[Fig. 3a](#)]. Thus, there is no need for non-constant velocities to compensate for the decreasing meniscus volume as blood is deposited. The quality of smears is also dependent on maintaining uniform contact between the spreader and sample slides — even a slight lift of the spreader will make the meniscus recede and hinder the wetting of the sample slide, therefore creating a non-uniform

smear with large zones of overlapping cells. In tests, we determine that no additional force or pressures is needed beyond the simple gravitational force on the spreader slide on the sample slide to produce the necessary continuous contact on the resulting wedge.

## **Inkwell design: Electricity-Free Blood Smearing**

Next, we focus on the design challenge to enable optimal smearing conditions experimentally established in previous section - in an electricity free 3D printed device that is easy to use and possible to replicate anywhere. Since the device is designed to make a perfect smear every time with no user experience - we term it “inkwell”. Designed for the most remote field sites, Inkwell is designed to be a low-cost and simple device that can “purely” mechanically (no batteries) recreate the exact optimal smearing parameters described above without the use of any motors or electricity. Intended to be used by non-experts, here we present design methodology for Inkwell with a focus on ease of use with minimal training for reliably and consistently producing high-quality smears of tunable thicknesses (and therefore tunable densities). As described below, all parts are made from easily accessible off-the-shelf components and simple 3D-printing approaches for reproducibility. For lack of space, we describe the design cycle and various prototypes in supplementary materials - while only focus on the final design output in detail below.

The final design of Inkwell has three main sub-assemblies: a static base, a carriage that holds the sample slide and translates along the base, and a spreader holder hinged on the base [Fig. 4c, d]. The key operation of Inkwell can be summarized as follows. For smooth operation with a constant velocity, we need a carriage and a linear spring coupled to a simple yet reliable dash pot. Here we achieve this by coupling a spiral spring with an air piston regulated by a simple valve as the only control knob for tuning. [Fig. 4b]. Once a linear carriage is pushed in and released manually by the user, a constant force spring coupled with an air piston and a regulating valve pushes the carriage back out to its initial position at a constant velocity [Fig. 4b]. This outward motion allows the spreader slide to smear

the blood across the sample slide. Although initially set to 15-20mm/s, the regulating valve is an adjustable needle valve which lets the user to precisely set the overall smear velocity as needed. The piston is an empty single-use plastic syringe specifically repurposed for our application. Using a syringe and valve combination as an adjustable air damper is novel and dramatically reduces the cost compared to traditional dashpots. See [Fig. 4a](#) for diagrams and a complete parts list.

Inkwell is easy to make and quick to assemble. It requires only a pair of flush wire cutters and a screwdriver. Teaching somebody how to assemble an Inkwell takes 15 to 20 minutes. Assembly of one unit takes 10 minutes for a newly trained person and 5 minutes for an experienced person. A step-by-step video guide for assembly is provide in supplementary video S6.

**Device operation** [[Fig. 5a](#) and [video S2](#)] Inkwell automates the technically-difficult aspects of producing a good thin smear while still giving the operator control and flexibility over smear thickness and length. We designed and tested Inkwell to operate on various slide brands - we successfully fitted and tested Inkwell with 13 different slide brands spanning 1 mm variation in width and length and 0.25 mm variation in thickness. Therefore any standard slide measuring roughly  $76 \times 26 \times 1 \text{ mm}^3$  will be suitable.

The operation of Inkwell is shown in [Fig. 5a](#). Make sure the carriage is extended out before starting the smearing process:

1. Place a clean sample slide in the carriage. Where applicable, the frosted surface (for slide labeling) should be facing up and outward (toward the outer edge of the device).
2. Insert a spreader slide in the spreader holder, with one of its long (75 mm) edges resting down on the sample slide (make sure the two slides make contact with each other). If the spreader slide has a frosted end, shift the spreader slide so that none of the frosted zone is in contact with the sample slide because that area impedes wetting.
3. Deposit a sample droplet of blood onto the sample slide over the marked area ( 25mm

from the end of the sample slide). We recommend 4  $\mu\text{L}$  measured using a pipette or an inverted cup[31, ?, 32].

4. While holding the base down securely with one hand, push the carriage toward the center of the device with the thumb of the other hand to wind the spring. Take care not to perturb the sample slide. Stop pushing once the drop fully contacts the spreader and spreads across the entire width of the sample slide. Waiting one to five seconds in this position may ensure the droplet is fully spread across the slide before proceeding.
5. Remove your thumb to allow the carriage to spring back out at the preset velocity. This motion automatically produces a thin smear.
6. Rotate the spreader along its hinge away from the sample slide and remove the spreader slide, then remove the sample slide.

A single spreader slide has four usable 75-mm edges, therefore can be used to make four separate smears. Between uses, ensure spreader edge is not already contaminated with previous blood samples. The spreader slide can then be cleaned with methanol and reused.

**Device performance** We assessed Inkwel’s performance by producing over one hundred whole blood smears in the lab with the single device. In order to test for usability, we asked three lab members, who were newly-trained on Inkwel, to produce thin smears using whole blood from five different samples. [Fig. 5b](#) shows photos of some of the resulting smears (with an initial volume of 4  $\mu\text{L}$  of whole blood). Regardless of the skill level of the operator, Inkwel can reliably produce high-quality thin smears using whole blood.

We also compared the smears made with Inkwel against conventional manual smears collected from the field in Uganda and Tanzania. As is generally known, field created smears done manually vary widely in quality and cell density, as is well documented [2]. For this study we chose two that were representative of the 40 smears collected. Using Octopi, our automated scanning microscope[6], we were able to scan entire smears and stitch them into a

**Table 1** Manual Vs. Inkwell Smears: Quality Comparison

Metric	Manual Smear (Uganda)	Inkwell Smear (Lab)
Maximum cell density (cells/mm <sup>2</sup> )	11,000	18,000
Monolayer area	20–40 %	97–99 %
Average cell density (cells/mm <sup>2</sup> )	2,800–4,400	13,000–16,000
Total distinguishable cells	2.8–4.4 million	13–16 million

gigapixel scan [supplementary scans S1-S4]. We then measured RBC density in each field of view with Cellpose [33]. These quantitative measurements demonstrated two advantages of smears made with Inkwell compared to typical hand smears from the field. Firstly, Inkwell produces much more uniform smears, with at least 80 percent of the slide covered in a monolayer. Secondly, Inkwell smears are much denser in the monolayer region, reaching 18,000 RBCs per mm<sup>2</sup> in some regions, which is the optimal density before cells start to overlap (see Methods section). Fig. 6 shows the example scans of Inkwell and manual field smears, with a corresponding heat map of the RBC density distribution across the slide. The gigapixel images for the Inkwell scans show up to 16 million distinguishable RBCs in a single image. To the best of our knowledge, this is the highest number of cells imaged on a single glass slide. There also is an average of up to 16,000 RBCs / mm<sup>2</sup>, corresponding to 89% density compared to optimal hexagonal packing across an entire slide [Supplementary scan S1], which is also unprecedented. In total, Inkwell can produce smears with about five times the number of distinguishable RBCs compared to the traditional manual smears we collected. See Table 1 for a summary of the quantitative comparison.

With Inkwell smears made almost entirely of a monolayer, microscopists and automated diagnostic systems can scan almost anywhere throughout the slide. This contrasts the reliance on the feathered edge zone in conventional smears. Macroscopically, this results in a notable difference between conventional smears which have a tongue-shaped feathered edge and smears made with Inkwell which cover a rectangular area.

## Repeatability, robustness, and lifetime testing

To assess Inkwell’s durability over time, we built a motorized stress-testing rig that simulates an operator repeatedly making smears over and over again. Once an Inkwell unit is placed into the rig, a stepper motor and an extended arm repeatedly push and release the carriage to simulate an operator’s hand [figS9, Video S4.A]. We test the device for a total of 10,000 cycles. To test performance, thin smears using whole blood before and after 10,000 cycles and the smear qualities between the two are comparable directly [Fig. 7a, b]. Even after undergoing 10,000 cycles there was almost no loss of functionality (in terms of velocity and smoothness of travel) [Fig. 7c]. It’s worth noting that after thousands of cycles the oil on the syringe barrel and seal gradually migrates away [18] which slowly increases friction and reduces the smear velocity (supplementary video S4.B). However this loss in velocity can be compensated by minimally opening the air valve. If, after many more cycles, friction becomes too high, then more oil can easily be added by removing the plunger. This maintenance operation takes about one minute.

**Usability study** A preliminary usability study was conducted in our lab and performed by four lab members to get initial feedback on Inkwell (see Materials and Methods for details). Overall, based upon the post-training survey responses, most participants found Inkwell easy to use and all produced better smears when using Inkwell compared to the conventional method by hand [Fig. 8b-d]. Most would consider using Inkwell to produce a large throughput of smears [Fig. 8e]. While the current usability study training did not include details on how to properly maintain and repair the device, hence the 50/50 split in confidence level amongst the participants’ response to being able to fix the unit [Fig. 8f], future training will include such details. Furthermore, a larger usability study with at least 20 field partners and 100 Inkwell units is currently in the planning phase.

## Discussion

The overall design of Inkwell over the years has undergone over forty iterations with testing and feedback from users around the world. These iterations range from an all-3D-printed device (including the spring) to motorized systems to ultra-simple compliant mechanisms. However, many of these iterations did not produce the repeatable high-quality smears that we stated as the early goal. Each iteration was tested with pseudo and whole blood and improvements were made in a step-wise manner. Some of the improvements include ways to reduce friction, the number of parts, and the overall assembly time and cost. This iterative process led to [Fig. 4] as the final design.

One of the main challenges in designing a smearing device such as Inkwell is to ensure carriage motion remains smooth and uniform throughout its life, i.e. thousands to tens of thousands of smears. This goal can be in conflict with lowering manufacturing costs, as cheaper parts tend to be less durable. In particular, the \$ 0.17 syringe we use as an air damper is critical to keep the price of Inkwell low but it is normally manufactured for single use [34]. Keeping the inside surface of the syringe barrel pristine and well-lubricated ensures a long lifespan for Inkwell. For this, care should be taken during assembly to not damage or scratch the inside of the syringe and that no contaminants should enter it. In final design, the metal spring, which unspools into the syringe, is mounted with enough clearance with the inside of the barrel in order to avoid scratching the surface. Furthermore, extra silicone oil lubricant is applied to the syringe plug during assembly. See supplementary video S8, where the top device has no extra oil and the bottom device does. Inadequate lubrication can also lead to the carriage jamming halfway or having stick-slip behavior. This leads to non-uniform smears, as shown in Fig. 5b (third and fourth smears from the left) which were made with inadequately lubricated devices.

With over 144 million thin smears examined per year [35] for diagnostic purposes. This demonstrates the large need for a low cost device like Inkwell. It is simple to enable multiple smear-making on a single Inkwell (per maneuver) to increase overall smear-making through-

put in the field. The current Inkwell device costs 20 dollars in parts - where majority of the cost is driven by 3D printing [2](#). In large scale using plastic molding, the price can be brought down to as low as 5 dollars per unit.

To further test Inkwell and it's use in real-world settings, we're currently producing 100 Inkwell devices (using filament 3D-printing, see Supplementary fig S3) to deploy to our field partners and garner feedback on Inkwell's ease of use, ease of maintenance, durability over multiple uses, and quality of smears produced by those working on the ground.

The role of 3D printing within the scientific and medical communities has grown and matured over the last decade in terms of precision, quality, and impact. Groups such as OpenFlexture [\[36\]](#) and Open Labware [\[37, 38\]](#) have compiled various high-quality, open-source designs that are applicable for use in microscopes, micromanipulators, and small-volume liquid handlers. The ability for anyone and anywhere in the world to build quality tools given a simple 3D printer significantly and unprecedentedly improves access to science and research including low resource and remote settings. The design of Inkwell is open-source and will contribute to this large body of work around fabrication and science to improve point-of-care diagnostics including malaria around the world.

## Materials and Methods

### Samples

Conventional smears were observed in the field in Uganda, Tanzania, and India. Conventional smears in the lab were made using five different samples of human whole blood with EDTA or heparin anticoagulant agents collected from the Stanford Blood Center, and with finger prick blood in the lab. Our motorised parameter sweep study was done with EDTA whole blood from the Stanford Blood Center. Inkwell smears were done in three different settings: (1) in a lab in Uganda with whole blood containing heparin anticoagulant agent, (2) in our Stanford lab with the five samples from the Stanford Blood Center noted above, and (3) in



our Stanford lab with fresh finger prick blood.

## **High-speed imaging of the smearing Process**

To understand the blood-smearing process microscopically, we observed the effects of the smearing action using a custom-built inverted microscope (Squid framework[39]) in a bio-safety cabinet at 600 fps. In this setup we used an 10x/0.25 objective corrected for 1.1 mm glass thickness, a 75 mm imaging lens as tube lens and an Imaging Source DMK 33UX252 camera. A schematics of the setup can be found in supplementary figure S4 f-g.

## **Design of the motorized characterization setup**

The design of our motorized experimental smearing setup is shown supplementary figure S4 e-g, consisting of 3D-printed and laser-cut parts, a Nema-17 stepper motor with lead screw, and various screws and fasteners. Velocity-controlled prismatic motion is achieved through a 3D-printed carriage actuated by the motor with a TMC2209 motor driver which is controlled by an Arduino Due. There is a magnetic latch on the coupler between the motor and carriage which acts as a mechanical fuse in case the carriage gets pushed too far or is obstructed, and prevents aerosolization or shattered glass slides in the case of mechanical failure. The spreader slide is held in place by an interchangeable slide holder which prescribes the tilt angle (Fig. S4 d). We used 75x25 mm non-beveled slides (3x1 in) and smeared 40–50 mm along the slide, across the entire 25 mm width, leaving room for a potential frosted end for labelling. The spreader slide holder also has integrated flexures with adjustment screws to set the contact pressure with the sample slide. In these parameter-sweep experiments, we used whole human blood with EDTA or heparin anticoagulant. Blood droplet volume was controlled using a pipette.

## Inkwell Mechanical Design

According to the results from the parameter-sweep experiments, to generate a uniform monolayer of red blood cells, we need to drag the glass spreader across the sample slide at constant velocity along a straight line. The easiest way to passively achieve this is to oppose a constant traction force  $F_{spring}$  with a viscous damping force  $F_{damping}$ , much like how terminal velocity is reached by objects falling through a liquid under the action of gravity. By varying the viscous friction coefficient  $\alpha$ , we can adjust the terminal velocity and therefore the smear thickness. In the case of quadratic friction, this velocity is given by Newton’s second law applied to the spreader of mass  $m$  subject to these two forces:  $m\ddot{x} = F_{spring} - F_{damping} = F_{spring} - \alpha(s)\dot{x}^2$  which yields in steady state:  $\dot{x} = \sqrt{\frac{F}{\alpha(s)}}$  where  $x$  is the position of the spreader and  $s$  formalizes the parameter used to adjust the damping coefficient.

Inkwell has three main parts: (1) a static base, (2) a carriage that holds the sample slide and translates along the base, and (3) a spreader holder hinged on the base. Structural parts were 3D-printed out of PLA on a Prusa printer (i3 MK3S+). The carriage is actuated by a 500g constant force spring (i.e. a rolled metal strip that recoils when extended [40]) and dampened by a friction piston. As opposed to using a counterweight, the spring allows for a more compact design and avoids the need to redirect the weight’s vertical force. Furthermore, this constant force spring, unlike spiral springs found in e.g. mechanical watches or measuring tapes, at its resting state is recoiled rather than expanded, making the design even more compact. To dampen the spring’s motion, we use vacuum pressure in the form of a tunable airflow. Traditionally, this is done by using an expensive dashpot [41], an ultra-low friction graphite piston designed for smooth and constant dampening. For example commercial smear-making device, Hemaprep, uses a pair of dashpots for the same purpose. However, we found that a plastic syringe [34] with extra lubricant, fitted with a luer-lock adaptor and an adjustable needle valve, can provide comparable smooth dampening. Globally, tens of billions of plastic syringes are produced annually and at only a few cents per unit [42], compared to dashpots which cost as much as \$80 per unit. Using 17 cents syringe significantly

reduces the cost of Inkwell.

The needle valve can precisely regulate the amount of airflow and thus fine-tune the steady-state velocity of the carriage. The air reservoir volume between the syringe tip and the needle valve intake is kept as small as possible because the air trapped here expands and acts as a spring when the carriage extends out. As part of the design development, we also tested a variety of tubing (with varying diameters and malleability) that would connect the needle valve to the luer-lock and syringe. The optimal tubing was one that provided sufficient seal, easy to insert into both terminals, and resistant to buckling (to prevent blocking air-flow) (fig. S3 c).

Gravity and a level mechanism are sufficient to keep contact between the spreader slide and the sample slide. A spring-loaded mechanism to push the spreader down against the sample slide may over-constrain the translation motion and create unnecessary friction. Therefore the spreader holder is loosely hinged on the main body, giving it a little extra play so the edge of the spreader slide can conform to the surface of the sample slide and compensate for any misalignment of the carriage. This is much easier to design and manufacture and will perform much better than a perfectly aligned and constrained system. An over-constrained spreader holder might cause contact loss in case of slight misalignment. We found that the sample slide does not need to be so tightly fixed on the carriage: leaving 0.5 mm to 1 mm of play on each edge of the slide does not affect smear quality.

**BOM and cost** The exact part by part bill of materials for our prototype is given Table 2. Further reduction in per unit cost is easily possible with greater production volume, cheaper off-the-shelf parts, and alternative means of production. For example, injection plastic molding can reduce the cost of 3D printed parts from O(\$10) to O(\$1).

**Table 2** Inkwell BOM and Cost

Part	Cost at 10 units (USD)	Cost at 100 units (USD)
Set of 3D printed parts	\$ 8.50	\$ 7.50
3mm x 100mm rod (x2)	\$ 0.90	\$ 0.90
3mm x 25mm rod	\$ 0.20	\$ 0.20
Igus bearings (x2)	\$ 2.56	\$ 1.62
Constant force spring	\$ 6.45	\$ 3.20
Syringe	\$ 0.19	\$ 0.19
Syringe barb fitting	\$ 0.44	\$ 0.44
Rubber tube	\$ 0.08	\$ 0.08
Valve	\$ 0.74	\$ 0.50
M3 x 6mm screws (x2)	\$ 0.20	\$ 0.20
Total	\$ 20.26	\$ 14.83

## 2 Long-term durability testing

To test the long-term durability of Inkwell, we built a stress-testing rig to simulate the usage of Inkwell over thousands of cycles (fig. S9). The stress-testing rig fits two Inkwell units and can run the simulation in parallel. The rig has a stepper motor and arm that push and release the Inkwell unit(s) per cycle. The rig has adaptable mounting brackets and spacers to fit various versions of Inkwell prototypes. We tested our units 1,000 cycles at a time with an overnight pause between each session to account for mechanical wear and oil drying as seen in normal usage patterns. We found that a unit can withstand 10,000 cycles without any loss in functionality. At close to 20,000 cycles, the device occasionally jams. This can be remedied by loosening the valve and hand-operating the device a few times. If the jamming remains an issue, reapplying oil onto the syringe plunger removes the issue entirely. The predominant source of wear and variability is the gradual oil displacement in the syringe. Other elements like the slide holder have very little wear. Therefore the variation in velocity throughout a single smear (visible macroscopically as bands or multi-gradients within the smear) is sufficient to alert the user to adjust either the valve or reapply oil as necessary to maintain smear quality.

**Syringe lubrication** As noted above, re-lubrication of the syringe plunger may be necessary after thousands of continuous use cycles. We tested mineral oil (universal sewing machine oil) and silicone oil (100 cst viscosity) to smoothen the carriage motion. For this test, we applied the experimented oil on the syringe plunger during assembly (about 5-10  $\mu\text{L}$ ) and cycled the device until there was a noticeable increase in friction. We found that mineral oil dries relatively quickly and results in high stiction, whereas silicone oil last for tens of thousands of cycles and does not dry as easily. We also observed oil being wiped off whenever the plunger is removed for maintenance, therefore to prevent stiction, more oil needs to be reapplied each time the plunger is removed. Additionally, if the plug/rubber tip is pushed in all the way until it butts up against the inner tip of the syringe, the plunger can get stuck from oil making an internal wet seal and that excess oil by depositing into the inside tip of the syringe. Our current design has a built-in mechanical stop that prevents this from happening.

**Usability study** Since Inkwell was designed primarily for untrained, unskilled individuals, the four participants in a preliminary usability test were selected based on their inexperience with making thin blood smears [Fig. 8a]. The usability study was done in two identical sessions (two participants each) where participants were minimally trained on how thin blood smears are conventionally made and shown how to operate Inkwell to produce thin blood smears. Examples of “good” and “bad” smears were presented to each participant as part of the training. To eliminate the need for additional safety training on handling blood, a phantom blood solution (designed to mimic the rheological properties of human whole blood and was prepared according to IS 5405:1980) was used. Each participant was allowed to practice smear-making on roughly three to five slides, after which they are asked to produce five thin smears by hand and five thin smears using Inkwell. The initial volume of phantom blood was set at 4  $\mu\text{L}$  per smear. After producing the ten smears, each participant was given a short questionnaire to fill out [Fig. 8b-f]. The questions include rating their ability

to produce smears using Inkwell and the quality of smears by Inkwell in comparison to the conventional manual method. Additional questions ask participants to briefly describe any shortcomings or misunderstandings of the instructions and/or of the device, and whether they would consider using Inkwell for future fieldwork or not, and why.

## **Acknowledgements**

We thank the following individuals for participating in the Inkwell usability study: Ethan Li, Hope Leng, Grace Zhong, Ray Chang, and Jijumon A.S. We thank Ipsita Pal Bhowmick for discussions and images used in figure 1. We thank all members of the PrakashLab for fruitful discussions and comments. This work was funded by Gates Foundation Award (M.P), Schmidt Futures Innovation Fellowship (M.P) and Moore Foundation Research Grant (M.P.) and NSF CCC (DBI1548297 (M.P.)). M.P., H.L. and A.K. identified the research problem. M.P., A.K. and D.A. developed the initial prototypes and experiments. J.N. and A.K. developed prototypes and implemented the final Inkwell device with input from all authors. J.N., H.L. and A.K. set up the motorized smearing device for characterizations. H.L. set up the apparatus for high-speed imaging and the Octopi microscope for scanning the blood smears. J.N. and A.K. performed data collection. A.K. designed the usability studies. J.P. validated an earlier prototype in field settings. J.N., H.L., A.K., and M.P. wrote the manuscript with feedback from all authors.

## **Figures and Captions**

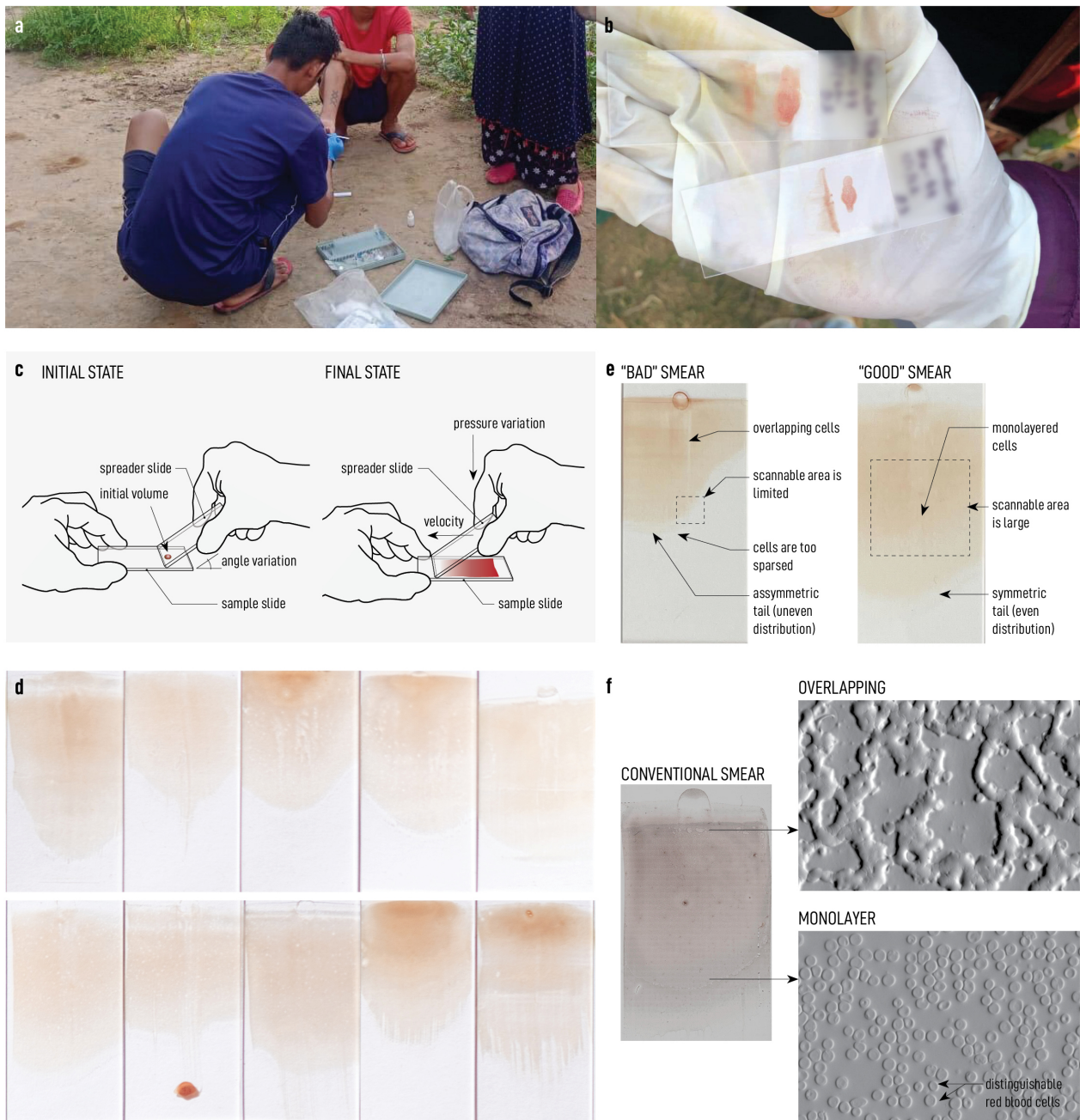


**Fig. 1 Variability commonly found in the quality of thin smears made by hand across different users.** [a] Field site conditions where healthcare workers visit patients door to door to collect blood samples and produce thin blood smears at the point of care. [b] Examples of typical smears produced in the field - many of which are of variable quality, resulting in inaccurate diagnoses for malaria or unreadable slides. [c] Schematic diagram showing how thin smears are made conventionally (by hand): first deposit a droplet of blood onto a sample slide, then make contact between the droplet and a spreader slide, and finally push the spreader slide across the sample slide to produce the smear. This manual method often yields in variability in angle between the two slides, velocity of the spreader slide, and pressure between the two slides, along with differences in initial droplet volume. [d] Thin smears produced by hand by lab members with varying levels of smear-making experience. [e] Some common characteristics that distinguish “good” from “bad” smears include symmetry and evenness of the smear (yielding to even distribution of monolayered cells).<sup>23</sup> [f] In conventional smears, there’s typically a zone with some overlapping cells and another with monolayered cells [f]. “Good” smears typically have larger monolayer zones, whereas “bad” smears are dominated with zones of overlapping cells.

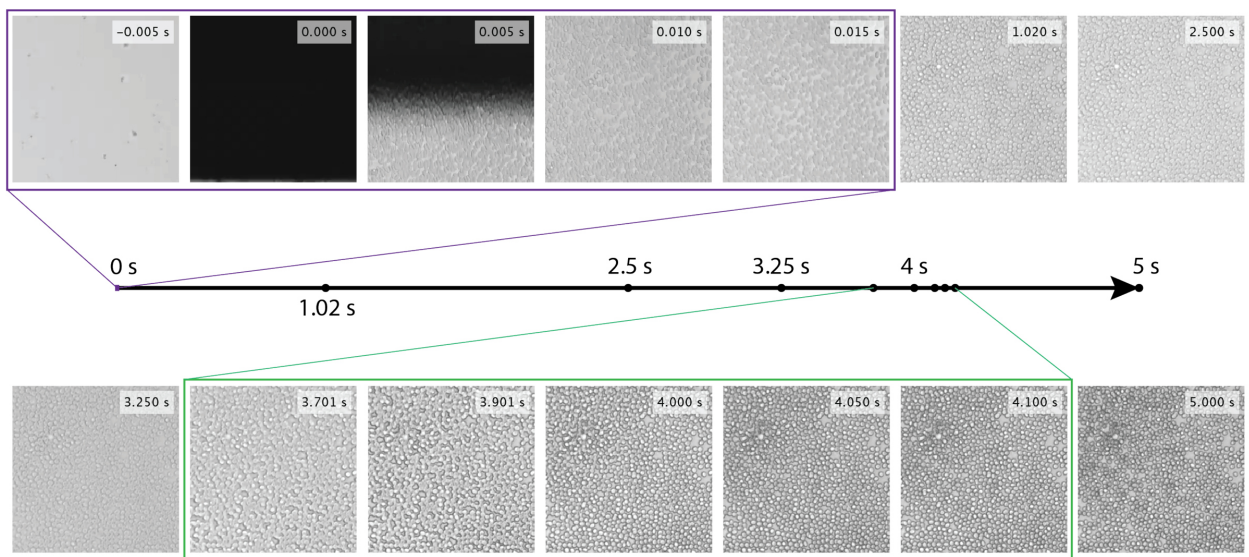


**Fig. 2 Blood film deposition process captured on a high-speed camera.** An array of images from the high-speed camera at various time points given an initial droplet volume of 3 $\mu$ L and with a velocity of 25mm/s. The images show the motion of the viscous red blood cells at their initial, settling, and dried states, clearly demonstrating various phases associated with the dynamics of thin film smear formation.



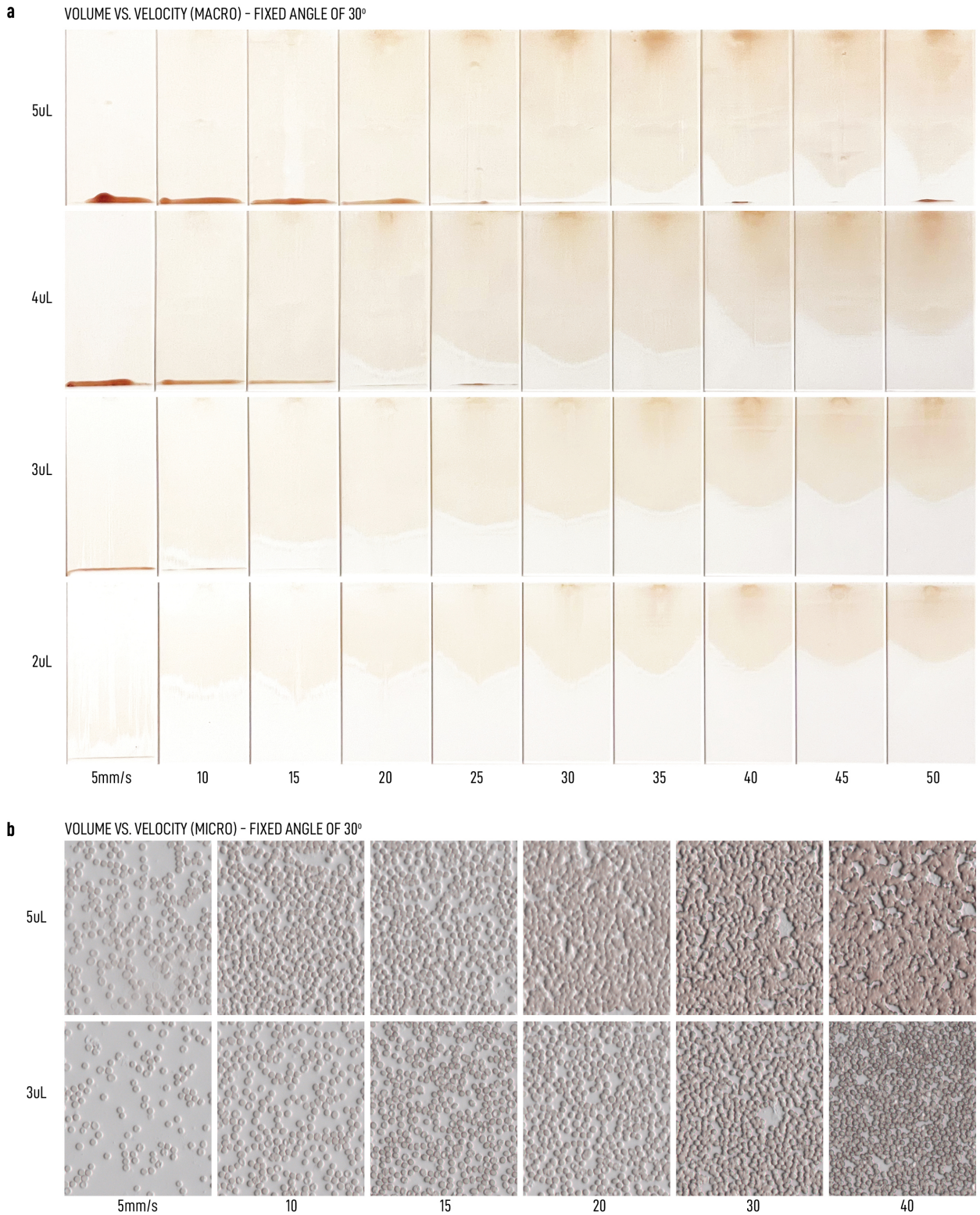


**Fig. 3 Analysis of the smears made under a set of controlled parameters.** [a] A macroscopic view of the array of thin smears produced using the characterization setup, given a fixed spreader angle of 30 degrees, while varying the initial blood droplet volumes (2  $\mu$ L, 3  $\mu$ L, 4  $\mu$ L, and 5 $\mu$ L) and the spreader velocities (5-50mm/s). [b] Representative microscopic fields of view for a subset of smears show the density and configuration of red blood cells given different parameters.

**a INKWELL BY COMPONENTS**

1. 3D-printed base
2. dowel pin 3mm x 25mm
3. 3D-printed spool holder
4. constant velocity spring
5. (2) M3 x 6mm
6. 3D-printed plunger
7. rubber syringe tip
8. 3D-printed carriage
9. sample slide
10. 5mL plastic syringe body
11. (2) 3mm dia. x 100mm steel rods
12. (2) sleeve bearings
13. 3D-printed spreader slide holder
14. spreader slide
15. 3/32" luer lock
16. tunable needle valve
17. flexible plastic tubing (ID 3/32")
18. 3D-printed cap

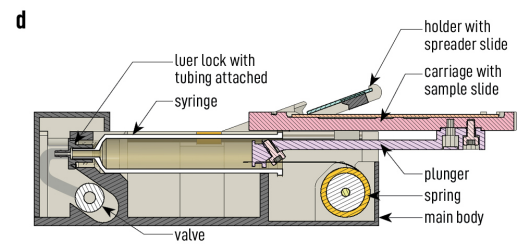
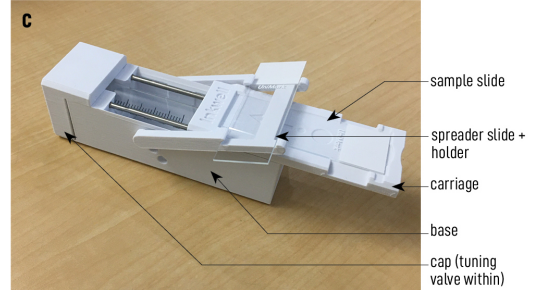
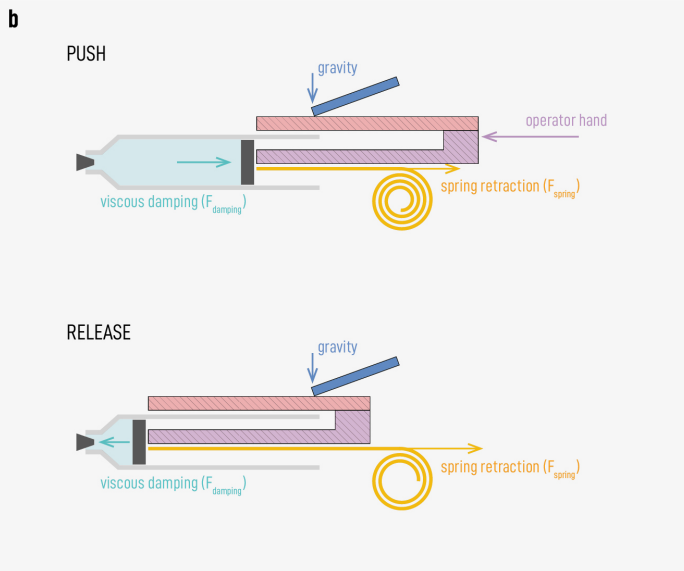
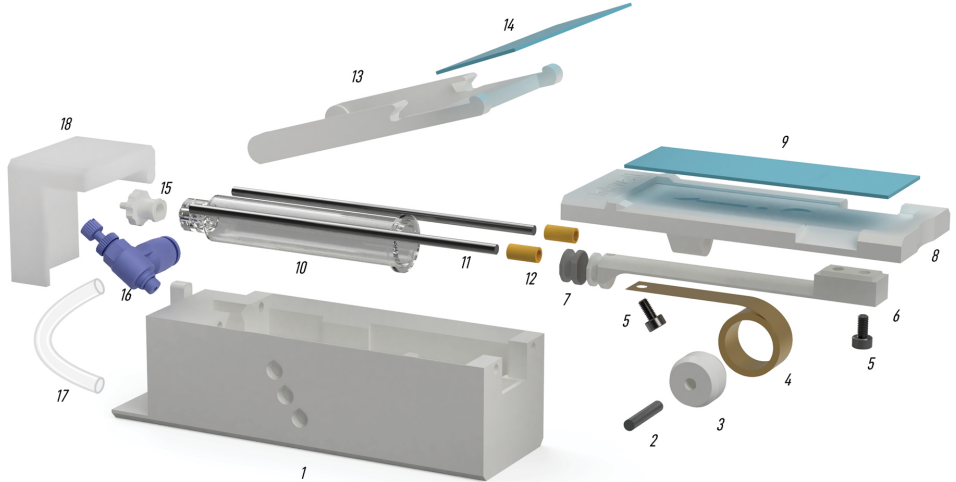
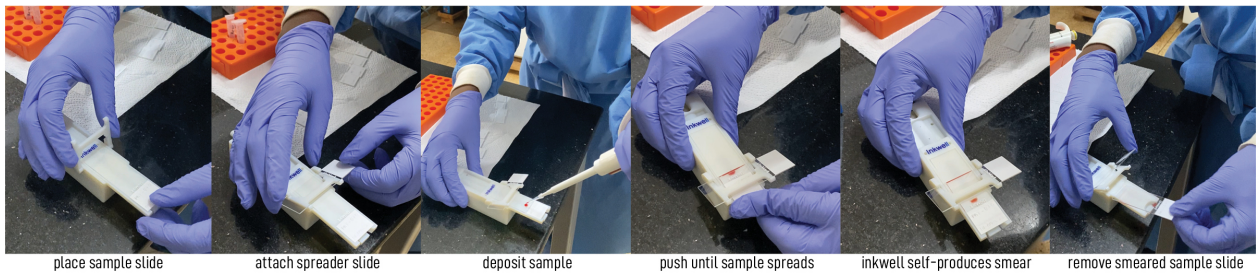
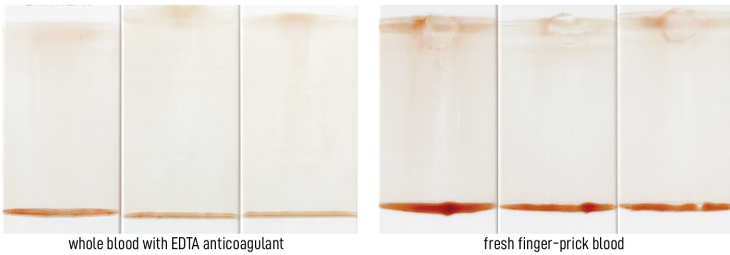


**Fig. 4 Inkwell design** [a] Exploded CAD diagram of Inkwell parts consisting of a series of 3D-printed components and off-the-shelf parts. [b] Sectional diagram showing the interactive forces at both the initial push state (user's manual force) and the latter release state (spring force and vacuum pressure). [c] The latest Inkwell design in lab. [d] CAD sectional diagram of Inkwell showing how the components fit within the unit.

**a** OPERATION OF INKWELL



**b** INKWELL SMEARS



**c** INKWELL SMEAR AT DIFFERENT MAGNIFICATIONS

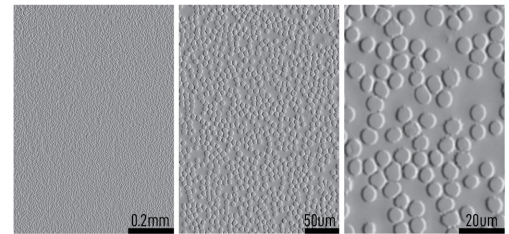
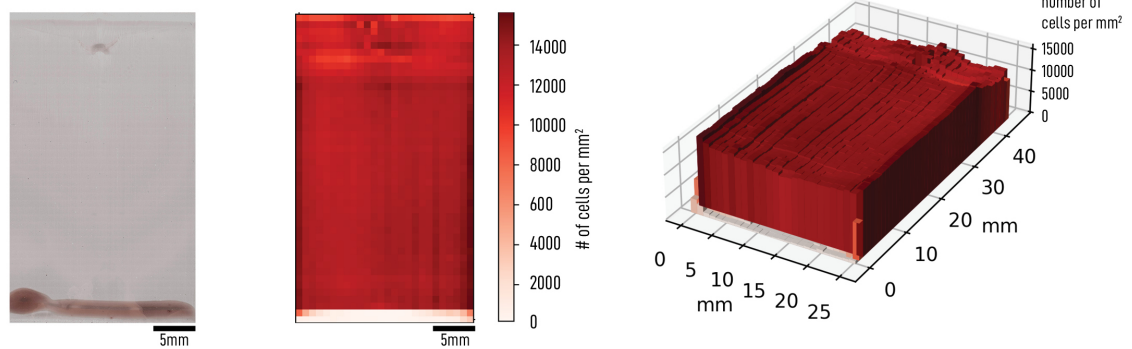
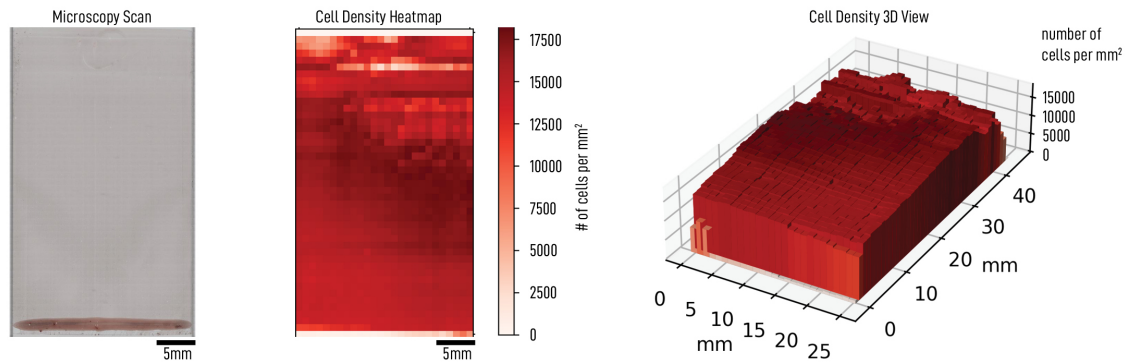


**Fig. 5 Functionality of Inkwell** [a] Step-by-step how-to photos of a technician using Inkwell to produce a thin smear. [b] Comparative array of thin smears produced using Inkwell at Stanford by a minimally-trained lab member using whole blood containing EDTA as anticoagulant versus fresh finger-prick blood. [c] Microscopic scan of a thin smear produced by Inkwell at 3 different magnifications showing the uniformity of density of monolayer of red blood cells.

**a** INKWELL SMEARS



**b** CONVENTIONAL SMEARS (BY HAND)

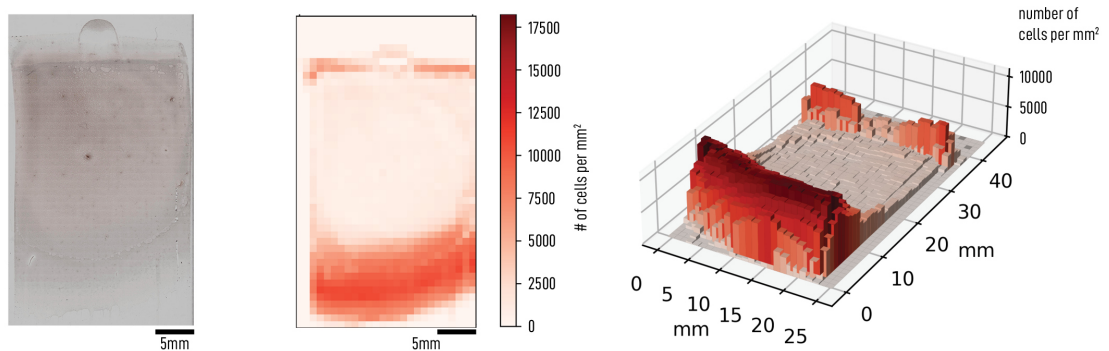
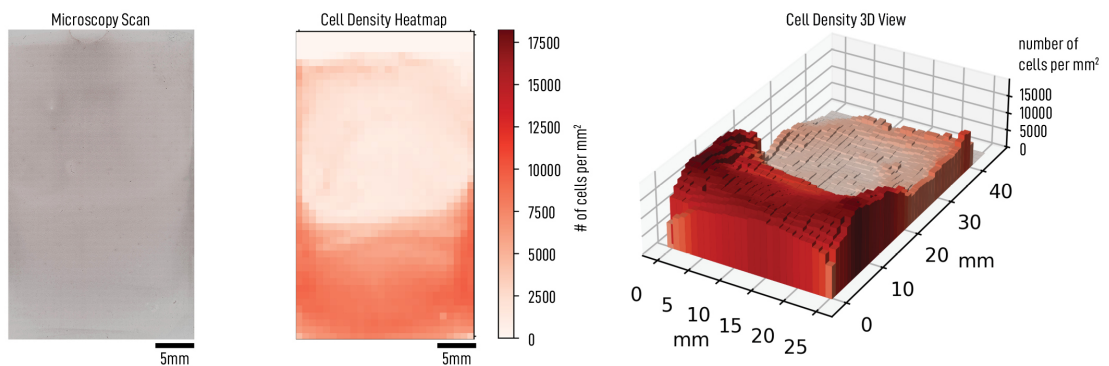


**Fig. 6 Evaluation of smears made with Inkwell** [a] Scans along with 2D heatmaps and a 3D representations of predicted per-field-of-view cell density of two selected thin-smears produced using Inkwell. [b] As a comparison, similar scans and cell density representations were done for two conventional smears made by hand.



**Fig. 7 Inkwell tested 10,000 cycles** To assess the robustness over time, Inkwell was subjected to multiple push-release cycles with the aid of a motorized system (see Materials and Methods). [a] Thin blood smears produced using two different Inkwell units, one newly assembled and another which had undergone 10,000 simulated cycles, were of comparable quality to each other. [b] Scans of the thin blood smears from [a] show comparable RBC densities. [c] Observed velocities across the two Inkwell units (left new, right after 10,000 test cycle run) show comparable motions of the carriage (a readout of uniform and consistent velocity) without reduction in smoothness.

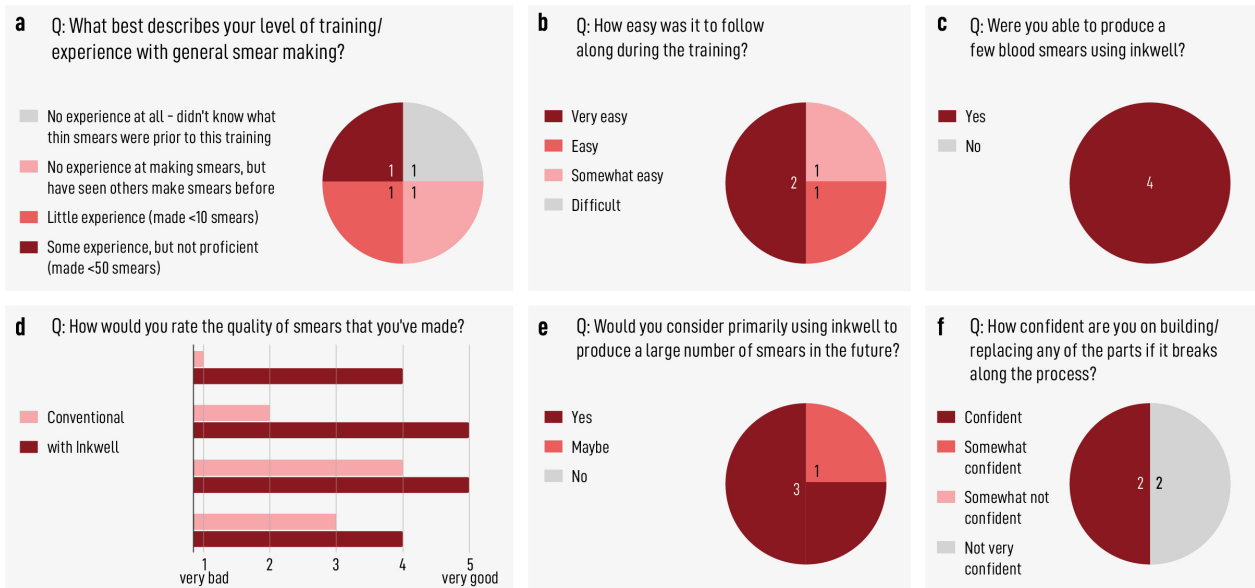


**Fig. 8 Inkwell usability survey** Questions and answers from the usability test survey that each volunteer was asked to fill out post the training session. [a] All four volunteers were selected for having little to no experience in making thin smears - the target user group for Inkwell. [b] Most participants noted that Inkwell was easy learn to use following the brief training. [c] All participants were able to produce smears using Inkwell. [d] All participants rated the smears produced using Inkwell exceed the quality of those produced conventionally by hand. [e] Most participants would consider using Inkwell to produce smears in the future, especially for high throughput. [f] Half of the participants were confident and the other half not in fixing or replacing any potentially broken elements of Inkwell. However, the training only demonstrated how to tune the velocity using the valve knob and did not cover how to fix broken parts.

## References

- [1] Organization, W. H. *Malaria microscopy quality assurance manual-version 2* (World Health Organization, 2016).
- [2] Sori, G., Zewdie, O., Tadele, G. & Samuel, A. External quality assessment of malaria microscopy diagnosis in selected health facilities in western oromia, ethiopia. *Malaria journal* **17**, 1–7 (2018).
- [3] Mutabazi, T. *et al.* Assessment of the accuracy of malaria microscopy in private health facilities in entebbe municipality, uganda: a cross-sectional study. *Malaria Journal* **20**, 1–9 (2021).
- [4] Guerin, P. J. *et al.* Malaria: current status of control, diagnosis, treatment, and a proposed agenda for research and development. *The Lancet Infectious Diseases* **2**, 564–573 (2002).
- [5] Organization, W. H. & for Disease Control, C. *Basic malaria microscopy: tutor’s guide* (World Health Organization, 2010).
- [6] Li, H., Soto-Montoya, H., Voisin, M., Valenzuela, L. F. & Prakash, M. Octopi: Open configurable high-throughput imaging platform for infectious disease diagnosis in the field. *BioRxiv* 684423 (2019).
- [7] Das, D. *et al.* Field evaluation of the diagnostic performance of easyscan go: a digital malaria microscopy device based on machine-learning. *Malaria Journal* **21**, 122 (2022).
- [8] Maguire, J. D. *et al.* Production and validation of durable, high quality standardized malaria microscopy slides for teaching, testing and quality assurance during an era of declining diagnostic proficiency. *Malaria Journal* **5**, 1–8 (2006).

- [9] Kahama-Maró, J., D'Acromont, V., Mtasiwa, D., Genton, B. & Lengeler, C. Low quality of routine microscopy for malaria at different levels of the health system in dar es salaam. *Malaria Journal* **10**, 1–10 (2011).
- [10] Harchut, K. *et al.* Over-diagnosis of malaria by microscopy in the kilombero valley, southern tanzania: an evaluation of the utility and cost-effectiveness of rapid diagnostic tests. *Malaria journal* **12**, 1–9 (2013).
- [11] Ngasala, B. & Bushukatale, S. Evaluation of malaria microscopy diagnostic performance at private health facilities in tanzania. *Malaria journal* **18**, 1–7 (2019).
- [12] for Disease Control, C. & Prevention. Specimen processing (2020). URL <https://www.cdc.gov/dpdx/diagnosticprocedures/blood/specimenproc.html>.
- [13] Organization, W. H. *et al.* *Basic malaria microscopy: Part I. Learner's guide*. Ed. 2 (World Health Organization, 2010).
- [14] Organization, W. H. *et al.* Collection of finger-prick blood and preparation of thick and thin blood films. Tech. Rep., World Health Organization (2016).
- [15] Adewoyin, A. Peripheral blood film-a review. *Annals of Ibadan postgraduate medicine* **12**, 71–79 (2014).
- [16] Moura, S. *et al.* Impact of a training course on the quality of malaria diagnosis by microscopy in angola. *Malaria Journal* **13**, 1–7 (2014).
- [17] AmScope. Globe scientific diamond perfect smear blood smearing tool. URL <https://amscope.com/collections/globe-scientific/products/c-vgsc-1300>.
- [18] Saad Albichr, I. *et al.* Cross-evaluation of five slidemakers and three automated image analysis systems: The pitfalls of automation? *International Journal of Laboratory Hematology* **42**, 573–580 (2020).



- [19] McDermott, S. *et al.* autohaem: 3d printed devices for automated preparation of blood smears. *Review of Scientific Instruments* **93**, 014104 (2022).
- [20] Sysmex. Seed haematology, sysmex educational enhancement and development. Tech. Rep., Sysmex (2013).
- [21] Sysmex. Ral stainer. URL <https://www.sysmex-mea.com/products/products-detail/ral-stainer.html>.
- [22] Britten, J. A. A simple theory for the entrained film thickness during meniscus coating. *Chemical Engineering Communications* **120**, 59–71 (1993).
- [23] Le Berre, M., Chen, Y. & Baigl, D. From convective assembly to landau-levich deposition of multilayered phospholipid films of controlled thickness. *Langmuir* **25**, 2554–2557 (2009).
- [24] Reznik, S., Salalha, W., Sorek, Y., Avramov, D. & Zussman, E. Entrainment of a film on a surface from the meniscus of a liquid wedge during coating. *Physics of Fluids* **21**, 102001 (2009).
- [25] Mayer, H. & Krechetnikov, R. Landau-levich flow visualization: Revealing the flow topology responsible for the film thickening phenomena. *Physics of Fluids* **24**, 052103 (2012).
- [26] Thurston, G. B. Viscoelasticity of human blood. *Biophysical journal* **12**, 1205–1217 (1972).
- [27] Errill, E. Rheology of blood. *Physiological reviews* **49**, 863–888 (1969).
- [28] Doumenc, F., Salmon, J.-B. & Guerrier, B. Modeling flow coating of colloidal dispersions in the evaporative regime: prediction of deposit thickness. *Langmuir* **32**, 13657–13668 (2016).

- [29] Gutenev, P., Pyatnitskii, A. & Klimova, N. Liquid entrainment from the meniscus of a liquid wedge by a moving horizontal plate. *Colloid Journal* **65**, 301–304 (2003).
- [30] Cheng, C. K.-W., Chan, J., Cembrowski, G. S. & van Assendelft, O. W. Complete blood count reference interval diagrams derived from nhanes iii: stratification by age, sex, and race. *Laboratory Hematology* **10**, 42–53 (2004).
- [31] Hopkins, H. *et al.* Blood transfer devices for malaria rapid diagnostic tests: evaluation of accuracy, safety and ease of use. *Malaria journal* **10**, 1–9 (2011).
- [32] Incardona, S. *et al.* The inverted cup device for blood transfer on malaria rdts: ease of use, acceptability and safety in routine use by health workers in nigeria. *Malaria Journal* **17**, 1–8 (2018).
- [33] Stringer, C., Wang, T., Michaelos, M. & Pachitariu, M. Cellpose: a generalist algorithm for cellular segmentation. *Nature methods* **18**, 100–106 (2021).
- [34] Scientific, F. Fisherbrand sterile syringes for single use. URL <https://www.fishersci.com/shop/products/sterile-syringes-single-use-12/14955458>.
- [35] Organization, W. H. *et al.* *World malaria report 2022* (World Health Organization, 2022).
- [36] Collins, J. T. *et al.* Robotic microscopy for everyone: the openflexure microscope. *Biomedical Optics Express* **11**, 2447–2460 (2020).
- [37] Baden, T. *et al.* Open labware: 3-d printing your own lab equipment. *PLoS biology* **13**, e1002086 (2015).
- [38] Amann, S., Witzleben, M. v. & Breuer, S. 3d-printable portable open-source platform for low-cost lens-less holographic cellular imaging. *Scientific reports* **9**, 1–10 (2019).
- [39] Li, H. *et al.* Squid: simplifying quantitative imaging platform development and deployment. *bioRxiv* 2020–12 (2020).

- [40] Ohtsuki, A., Ohshima, S. & Itoh, D. Analysis on characteristics of a c-shaped constant-force spring with a guide. *JSME International Journal Series C Mechanical Systems, Machine Elements and Manufacturing* **44**, 494–499 (2001).
- [41] Corp, A. Airpot. URL <https://www.airpot.com/free-samples-push-dashpot/>.
- [42] Radio, N. P. A looming challenge in the vaccination campaign: Syringe shortages (2021). URL <https://www.npr.org/2021/07/25/1020488395/a-looming-challenge-in-the-vaccination-campaign-syringe-shortages>.